

Arithmetic of arithmetic Coxeter groups

Suzana Milea^a, Christopher D. Shelley^b, and Martin H. Weissman^{a,1}

^aDepartment of Mathematics, University of California, Santa Cruz, CA 95064; and ^bPrivate address, Bolinas, CA 94924

Edited by Kenneth A. Ribet, University of California, Berkeley, CA, and approved November 16, 2018 (received for review June 3, 2018)

In the 1990s, J. H. Conway published a combinatorial-geometric method for analyzing integer-valued binary quadratic forms (BQFs). Using a visualization he named the “topograph,” Conway revisited the reduction of BQFs and the solution of quadratic Diophantine equations such as Pell’s equation. It appears that the crux of his method is the coincidence between the arithmetic group $PGL_2(\mathbb{Z})$ and the Coxeter group of type $(3, \infty)$. There are many arithmetic Coxeter groups, and each may have unforeseen applications to arithmetic. We introduce Conway’s topograph and generalizations to other arithmetic Coxeter groups. This includes a study of “arithmetic flags” and variants of binary quadratic forms.

arithmetic | Coxeter group | quadratic form | topograph

Binary quadratic forms (BQFs) are functions $Q: \mathbb{Z}^2 \rightarrow \mathbb{Z}$ of the form $Q(x, y) = ax^2 + bxy + cy^2$, for some integers a, b, c . The discriminant of such a form is the integer $\Delta = b^2 - 4ac$. In ref. 1, J. H. Conway visualized the values of a BQF through an invention he called the topograph.

1. Conway’s Topograph

The Geometry of the Topograph. The topograph is an arrangement of points, edges, and faces, as described below.

- Faces correspond to primitive lax vectors: coprime ordered pairs $\vec{v} = (x, y) \in \mathbb{Z}^2$, modulo the relation $(x, y) \sim (-x, -y)$. Such a vector is written $\pm \vec{v}$.
- Edges correspond to lax bases: unordered pairs $\{\pm \vec{v}, \pm \vec{w}\}$ of primitive lax vectors which form a \mathbb{Z} basis of \mathbb{Z}^2 . (Clearly this is independent of sign choices.)
- Points correspond to lax superbases: unordered triples $\{\pm \vec{u}, \pm \vec{v}, \pm \vec{w}\}$, any two of which form a lax basis.

Incidence among points, edges, and faces is defined by containment. A maximal arithmetic flag in this context refers to a point contained in an edge contained in a face. The geometry is displayed in Fig. 1; the points and edges form a ternary regular tree, and the faces are ∞ -gons. The group $PGL_2(\mathbb{Z}) = GL_2(\mathbb{Z})/\{\pm 1\}$ acts simply-transitively on maximal arithmetic flags.

On the other hand, the geometry of Fig. 1 also arises as the geometry of flags in the Coxeter group of type $(3, \infty)$. This is the Coxeter group with a diagram $\bullet \overset{3}{\text{---}} \bullet \overset{\infty}{\text{---}} \bullet$. The group W encoded by such a diagram is generated by elements $S = \{s_0, s_1, s_2\}$ corresponding to the nodes, modulo the relations $s_i^2 = 1$ (for $i = 0, 1, 2$), $s_0 s_2 = s_2 s_0$, and $(s_0 s_1)^3 = 1$. If $T \subset S$ is a subset of nodes, write W_T for the subgroup generated by T ; it is called a parabolic subgroup. The flags of type T are the cosets W/W_T . The Coxeter group W acts simply-transitively on the maximal flags; i.e., the cosets $W/W_\emptyset = W$.

The geometric coincidence reflects the fact that $PGL_2(\mathbb{Z})$ is isomorphic to the Coxeter group W of type $(3, \infty)$, a classical result known to Poincaré and Klein. But Conway’s study of lax vectors, bases, and superbases goes further, giving an arithmetic interpretation of the flags for the Coxeter group. This raises the natural question: Given a coincidence between an arithmetic group and a Coxeter group, is there an arithmetic interpretation of the flags in the Coxeter group?

Binary Quadratic Forms. If one draws the values $Q(\pm \vec{v})$ on the faces labeled by the primitive lax vectors $\pm \vec{v}$, one obtains Conway’s topograph of Q . Figs. 2 and 3 display examples. If u, v, e, f appear on the topograph of Q , in a local arrangement we call a cell, then Conway observes that the integers $e, u + v, f$ form an arithmetic progression.

$$\begin{array}{c}
 \diagup \quad u \quad \diagdown \\
 e \quad \quad v \quad f \\
 \diagdown \quad \quad \diagup
 \end{array}
 \quad f - (u + v) = (u + v) - e.$$

The discriminant of Q can be seen locally in the topograph, at every cell, by the formula $\Delta = u^2 + v^2 + e^2 - 2uv - 2ve - 2eu = (u - v)^2 - ef$.

A consequence of the arithmetic progression property is Conway’s climbing principle; if all values in a cell are positive, place arrows along the edges in the directions of increasing arithmetic progressions. Then every arrow propagates into two arrows; the resulting flow along the edges can have a source, but never a sink. This implies the existence and uniqueness of a well for positive-definite forms: a triad or cell which is the source for the flow. The well gives the unique Gauss-reduced form Q_{Gr} in the $SL_2(\mathbb{Z})$ -equivalence class of Q . More precisely, every well contains a triple $u \leq v \leq w$ of positive integers satisfying $u + v \geq w$, with strict inequality at triad wells and equality at cell wells (Fig. 2). Depending on the orientation of u, v, w at the well, the Gauss-reduced form is given below; in the ambiguously oriented case with $u = v$, $Q_{Gr}(x, y) = ux^2 + (u + v - w)xy + vy^2$. If $u + v = w$, both orientations occur in a cell well, and $Q_{Gr}(x, y) = ux^2 + vy^2$.

$$\begin{array}{c}
 \begin{array}{c}
 \diagdown \quad u \quad \diagup \\
 \circ \quad \quad \circ \\
 \diagup \quad \quad \diagdown
 \end{array}
 \quad \longmapsto \quad Q_{Gr}(x, y) = ux^2 + (u + v - w)xy + vy^2. \\
 \\
 \begin{array}{c}
 \diagup \quad u \quad \diagdown \\
 \circ \quad \quad \circ \\
 \diagdown \quad \quad \diagup
 \end{array}
 \quad \longmapsto \quad Q_{Gr}(x, y) = ux^2 - (u + v - w)xy + vy^2.
 \end{array}$$

When Q is a nondegenerate indefinite form, Conway defines the river of Q to be the set of edges which separate a positive

Significance

Conway’s topograph provided a combinatorial-geometric perspective on integer binary quadratic forms—quadratic functions of two variables with integer coefficients. This perspective is practical for solving equations and easily bounds the minima of binary quadratic forms. It appears that Conway’s topograph is just the first in a series of applications of arithmetic Coxeter groups to arithmetic. Four other applications are described in this article, and dozens more may be possible.

Author contributions: S.M., C.D.S., and M.H.W. designed research, performed research, analyzed data, and wrote the paper.

The authors declare no conflict of interest.

This article is a PNAS Direct Submission.

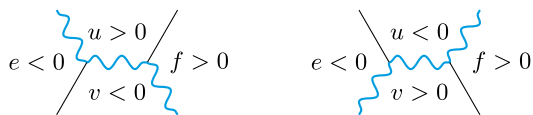
Published under the PNAS license.

¹To whom correspondence should be addressed. Email: weissman@ucsc.edu.

Published online December 26, 2018.

value from a negative value in the topograph of Q . Since all values on the topograph of Q must be positive or negative, the river cannot branch or terminate. The climbing principle implies uniqueness of the river. Thus, the river is a set of edges composing a single endless line. Bounding the values adjacent to the river implies periodicity of values adjacent to the river and thus the infinitude of solutions to Pell's equation. This is described in detail in ref. 1.

Riverbends—cells with a river as drawn below—correspond to Gauss's reduced forms in the equivalence class of Q .



Proposition 1. Let u, v, e, f be the cell values at a riverbend, with $e < 0, f > 0$. Then a Gauss-reduced form in the $SL_2(\mathbb{Z})$ -equivalence class of Q is given by

$$Q_{Gr}(x, y) = ux^2 + (u + v - e)xy + vy^2.$$

Proof: Let $b = (u + v) - e = f - (u + v)$ be the common difference at the cell. Then $Q_{Gr}(x, y) = ux^2 + bxy + vy^2$ is $SL_2(\mathbb{Z})$ equivalent to Q and we must prove Gauss's reduction conditions (ref. 2, article 183):

$$0 < b < \sqrt{\Delta} \text{ and } \sqrt{\Delta} - b < 2|u| < \sqrt{\Delta} + b.$$

Note that $0 < b$ since $e < f$. Since $b^2 - 4uv = \Delta$, and u and v have opposite sign, we find that $b^2 < \Delta$. Gauss's first reduction condition $0 < b < \sqrt{\Delta}$ follows.

Since $(u - v)^2 - ef = \Delta$, and e and f have opposite sign, we find that $\Delta > (u - v)^2$. Since u and v have opposite sign, this implies $\sqrt{\Delta} > \text{sgn}(u)(u - v)$. Multiplying by $4|u|$ yields $4|u|\sqrt{\Delta} > 4u(u - v)$. Replace $-4uv$ by $\Delta - b^2$ to obtain $4|u|\sqrt{\Delta} > 4u^2 + \Delta - b^2$. Rearranging yields

$$4u^2 - 4|u|\sqrt{\Delta} + \Delta < b^2.$$

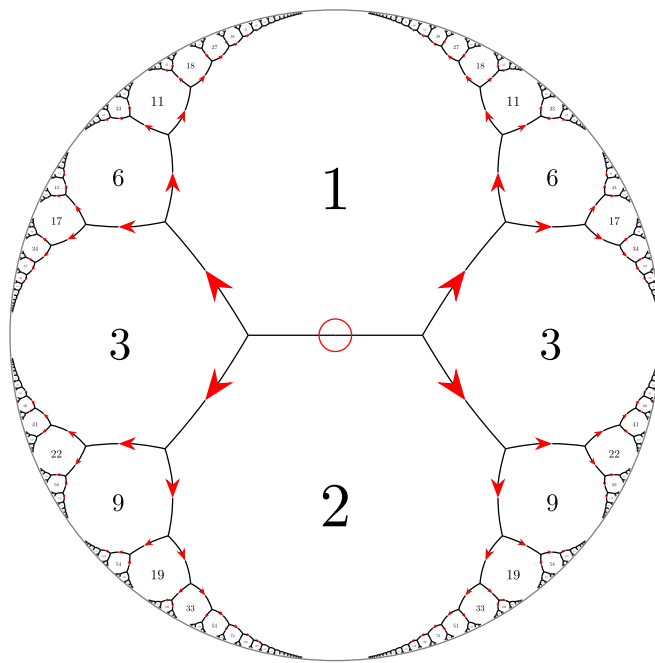


Fig. 2. The topograph of $Q(x, y) = x^2 + 2y^2$, with arrows exhibiting the climbing principle. The well (source of the flow) is the cell at the center.

Hence $(2|u| - \sqrt{\Delta})^2 < b^2$, and so $-b < 2|u| - \sqrt{\Delta} < b$. This verifies Gauss's second reduction condition. \square

The existence of riverbends gives a classical bound, by an argument we learned from Gordan Savin.

Theorem 2. The minimum nonzero absolute value μ_Q of a nondegenerate indefinite BQF Q satisfies $\mu_Q \leq \sqrt{\Delta/5}$.

Proof: At a riverbend, one finds $\Delta = (u - v)^2 - ef = u^2 + v^2 - uv - vu - ef$, the sum of five positive integers. It follows that one of $u^2, v^2, -uv, -vu, -ef$ must be bounded by $\Delta/5$. Among $|u|, |v|, |e|, |f|$, one must be bounded by $\sqrt{\Delta/5}$.

These are some highlights and applications of Conway's topograph. In the next sections, we describe generalizations.

2. Gaussian and Eisenstein Analogues

Let \mathbb{G} denote the Gaussian integers: $\mathbb{G} = \mathbb{Z}[i]$. Let \mathbb{E} denote the Eisenstein integers: $\mathbb{E} = \mathbb{Z}[e^{2\pi i/3}]$.

Arithmetic Flags and Honeycombs. One may generalize Conway's vectors, bases, and superbases to arithmetic structures in \mathbb{G}^2 and \mathbb{E}^2 . Guiding this are embeddings of $PSL_2(\mathbb{G})$ and $PSL_2(\mathbb{E})$ into hyperbolic Coxeter groups. In ref. 3, sections 1.I, 1.II, 3, and 6, Bianchi describes generators for $SL_2(\mathbb{G})$ and $SL_2(\mathbb{E})$ and fundamental polyhedra for their action on hyperbolic 3-space. Using reflections in the faces of these polyhedra, one may write explicit presentations of these groups; Fricke and Klein carry this out for $SL_2(\mathbb{G})$ in ref. 4, section I.8, where one finds a connection to the (later-named) Coxeter group of type $(3, 4, 4)$. Schulte and Weiss give a detailed treatment, proving the following in ref. 5, theorems 7.1 and 9.1.

Theorem 3. $PSL_2(\mathbb{G})$ is isomorphic to an index-two subgroup of $(3, 4, 4)^+$. $PSL_2(\mathbb{E})$ is isomorphic to an index-two subgroup of $(3, 3, 6)^+$.

Here $(a, b, c)^+$ denotes the even subgroup of the Coxeter group of type (a, b, c) . As the Coxeter groups of types $(3, 4, 4)$

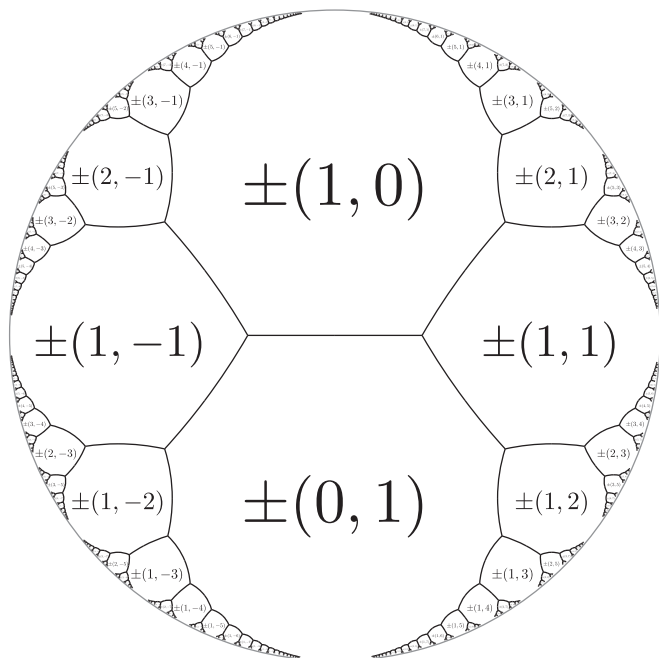


Fig. 1. Conway's geometry of primitive lax vectors, lax bases, and lax superbases.

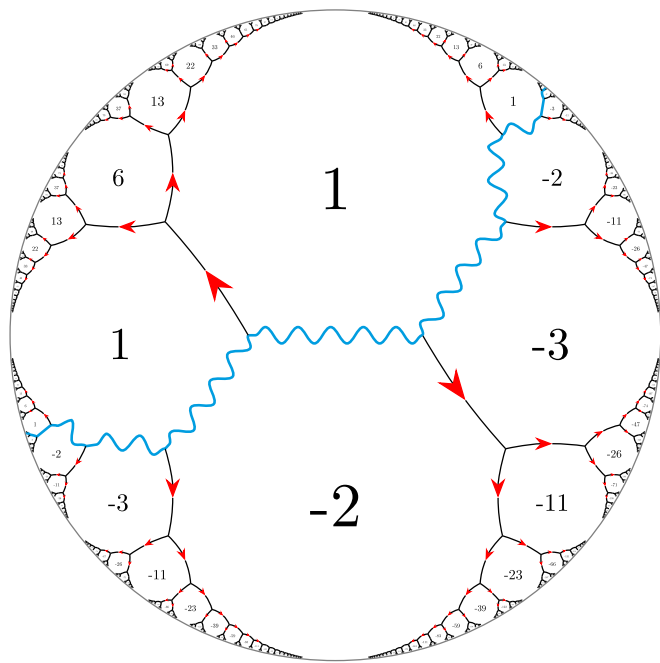


Fig. 3. The topograph of $Q(x, y) = x^2 - 3y^2$, exhibiting a periodic river. Solutions to Pell's equation $x^2 - 3y^2 = 1$ are found along the riverbank.

and $(3, 3, 6)$ are commensurable to $PSL_2(\mathbb{G})$ and $PSL_2(\mathbb{E})$, respectively, we expect an arithmetic interpretation of the Coxeter geometries. Such an arithmetic incidence geometry is described below.

- Cells correspond to primitive lax vectors: coprime ordered pairs $\vec{v} = (x, y) \in \mathbb{G}^2$ (respectively \mathbb{E}^2), modulo the relation $(x, y) \sim (\epsilon x, \epsilon y)$ for all $\epsilon \in \mathbb{G}^\times$ (resp., $\epsilon \in \mathbb{E}^\times$).
- Faces correspond to lax bases: unordered pairs $\{\epsilon\vec{v}, \epsilon\vec{w}\}$ of primitive lax vectors which form a \mathbb{G} basis of \mathbb{G}^2 (respectively \mathbb{E} basis of \mathbb{E}^2).
- Edges correspond to lax superbases: unordered triples $\{\epsilon\vec{u}, \epsilon\vec{v}, \epsilon\vec{w}\}$, any two of which form a lax basis.
- Points of the Eisenstein topograph* correspond to lax tetrabases: unordered quadruples $\{\epsilon\vec{s}, \epsilon\vec{t}, \epsilon\vec{u}, \epsilon\vec{v}\}$, any three of which form a lax superbasis.
- Points of the Gaussian topograph correspond to lax cubases: sets of three two-element sets $\{\{\epsilon\vec{u}_1, \epsilon\vec{u}_2\}, \{\epsilon\vec{v}_1, \epsilon\vec{v}_2\}, \{\epsilon\vec{w}_1, \epsilon\vec{w}_2\}\}$, such that all eight choices of $i, j, k \in \{1, 2\}$ give a lax superbasis $\{\epsilon\vec{u}_i, \epsilon\vec{v}_j, \epsilon\vec{w}_k\}$.

Incidence is given by the obvious containments described above. We call this incidence geometry the topograph for \mathbb{E} or \mathbb{G} , and it is equipped with an action of $PSL_2(\mathbb{E})$ and $PSL_2(\mathbb{G})$, respectively. The terms tetrabasis and cubasis reflect the residual geometry around a point (Fig. 4). Both geometries produce regular hyperbolic honeycombs (ref. 6, chap. IV); the points, edges, and faces around each cell form square or hexagonal planar tilings in the Gaussian or the Eisenstein case, respectively.

The Gaussian and Eisenstein topographs are described by Bestvina and Savin in ref. 7, sections 7 and 8. Both topographs, and the following link to Coxeter geometries, are given in the PhD thesis of the second author (8).

*The Eisenstein topograph was first described in 2007, in the unpublished master's thesis of Andreas Weinert.

Theorem 4. The topographs for \mathbb{E}^2 and \mathbb{G}^2 are equivariantly isomorphic to the Coxeter geometries of types $(3,3,6)$ and $(3,4,4)$, respectively.

By equivariance, we mean that the isomorphism intertwines the natural actions of $PSL_2(\mathbb{E})$ and $PSL_2(\mathbb{G})$ on one hand with the actions of the Coxeter groups on the other, via the inclusion described in Theorem 3.

Binary Hermitian Forms. An integer-valued binary Hermitian form (BHF), over \mathbb{E} or \mathbb{G} , is a function $H : \mathbb{E}^2 \rightarrow \mathbb{Z}$ or $\mathbb{G}^2 \rightarrow \mathbb{Z}$, of the form

$$H(x, y) = ax\bar{x} + \beta\bar{x}y + \bar{\beta}x\bar{y} + cy\bar{y}.$$

Here we assume $a, c \in \mathbb{Z}$, and $\beta \in (1 - \omega)^{-1}\mathbb{E}$ or $\beta \in (1 + i)^{-1}\mathbb{G}$ (the inverse different of \mathbb{E} or \mathbb{G} , respectively). The discriminant of H is the integer defined by

$$\Delta = (3 \text{ or } 4) \cdot (\beta\bar{\beta} - ac), \text{ for } \mathbb{E} \text{ or } \mathbb{G}, \text{ respectively.}$$

Fricke and Klein discuss reduction theory of Hermitian forms over \mathbb{G} , using the geometry of $SL_2(\mathbb{G})$, in ref. 4, section III.1,1–8. The topographs give a new approach, pursued by Bestvina and Savin (7).

Let H be a BHF over \mathbb{E} or \mathbb{G} . Recalling that cells of the topographs correspond to primitive lax vectors, we define the topograph of H to be the result of placing the value $H(\epsilon\vec{v})$ at the topograph cell marked by the primitive lax vector $\epsilon\vec{v}$. The most interesting case occurs when H is nondegenerate indefinite (taking positive and negative values, but never zero on a nonzero vector input). In this case, Conway's river is replaced by the ocean—the set of faces separating a cell with positive value from one with negative value. Bestvina and Savin prove (ref. 7, theorems 5.3 and 6.1) that this ocean is topologically an open disk, locally CAT(0) as a metric space, and the unitary group $U(H)$ acts cocompactly on the ocean.

Reduced indefinite BQFs correspond to riverbends in Conway's topograph. In a similar way, one finds reduced indefinite BHF's at the points of the ocean of negative curvature, i.e., where more than four ocean squares (for \mathbb{G}) or more than three ocean hexagons (for \mathbb{E}) meet at a point. From this, Bestvina and Savin (ref. 7, theorem 8.7) recover the optimal bound on the minima of nondegenerate indefinite BHF's over \mathbb{E} . The bound for \mathbb{G} can be obtained by the same method.

Theorem 5. Let H be a nondegenerate indefinite BHF. Then the minimum nonzero absolute value μ_H satisfies $\mu_H \leq \sqrt{\Delta/6}$.

Proof: The Eisenstein case is proved in ref. 7, so we prove the Gaussian case. Consider a vertex at which the ocean of H has negative curvature; such a point exists by ref. 7, corollary 6.2. The residue of the topograph at this vertex is a cube, whose faces are labeled by the values of H . The intersection of the ocean with

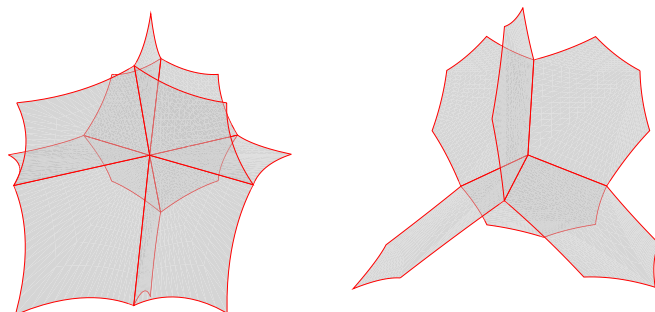
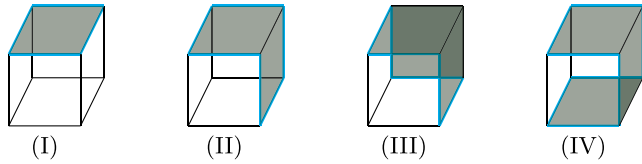


Fig. 4. The geometry of the Gaussian and Eisenstein topographs, displaying square and hexagonal faces and cubic and tetrahedral residues at a point.

this cube forms a simple closed path on the edges, separating positive-valued faces from negative ones.



Form I corresponds to a Euclidean vertex; forms II, III, and IV correspond to ocean vertices of negative curvature. Label the values of H on the cube by a, b, c, u, v, w , with a opposite u , b opposite v , and c opposite w . In ref. 7, proposition 7.1, Bestvina and Savin demonstrate that $a + u = b + v = c + w$. This excludes form IV, since the sum of two positive numbers cannot equal the sum of two negative numbers. Ref. 7, section 7 also gives a formula for the discriminant,

$$\Delta = z^2 - 2au - 2bv - 2cw, \text{ where } z = a + u = b + v = c + w.$$

In forms II and III, we may place a, u, b, v so that a and u have opposite signs, and b and v have opposite signs. Expressing z as $c + w$ yields

$$\Delta = c^2 + w^2 - 2au - 2bv.$$

As the right side is a sum of positive terms, we find

$$\min\{|a|, |b|, |c|, |u|, |v|, |w|\} \leq \sqrt{\Delta/6}.$$

□

3. Real Quadratic Arithmetic

Dilinear Algebra. Here we introduce a family of “dilinear groups” associated to certain real quadratic rings. Let $\sigma > 1$ be a square-free positive integer, and let $R_\sigma = \mathbb{Z}[\sqrt{\sigma}]$ be the quadratic ring of discriminant 4σ . We define the dilinear group $DL_2(R_\sigma)$ to be the group of all matrices $\begin{pmatrix} a & b \\ c & d \end{pmatrix} \in GL_2(R_\sigma)$ such that

$$(a, d \in \mathbb{Z} \cdot \sqrt{\sigma} \text{ and } b, c \in \mathbb{Z}) \text{ or } (a, d \in \mathbb{Z} \text{ and } b, c \in \mathbb{Z} \cdot \sqrt{\sigma}).$$

Let $DL_2^+(R_\sigma)$ denote its subgroup consisting of matrices with $a, d \in \mathbb{Z}$ and $b, c \in \mathbb{Z} \cdot \sqrt{\sigma}$. While the dilinear groups seem a bit mysterious at first, $DL_2^+(R_\sigma)$ is $GL_2(\mathbb{Q}(\sqrt{\sigma}))$ conjugate to a congruence subgroup of $GL_2(\mathbb{Z})$: If $g = \text{diag}(1, \sqrt{\sigma})$, then

$$gDL_2^+(R_\sigma)g^{-1} = \Gamma_0(\sigma) := \left\{ \begin{pmatrix} \alpha & \beta \\ \gamma & \delta \end{pmatrix} \in GL_2(\mathbb{Z}) : \gamma \in \sigma\mathbb{Z} \right\}.$$

We thank the referee for this insight.

A divector over R_σ will mean a vector in R_σ^2 of red or blue type. Red divectors are those of the form $(u, v\sqrt{\sigma})$ for some $u, v \in \mathbb{Z}$. Blue divectors are those of the form $(u\sqrt{\sigma}, v)$ for some $u, v \in \mathbb{Z}$. A red divector $(u, v\sqrt{\sigma})$ is called primitive if $\text{GCD}(u, \sigma v) = 1$. A blue divector $(u\sqrt{\sigma}, v)$ is called primitive if $\text{GCD}(u\sigma, v) = 1$.

Theorem 6. *The dilinear group $DL_2(R_\sigma)$ acts transitively on the set of primitive divectors, and $DL_2^+(R_\sigma)$ acts transitively on the set of primitive red (or blue) divectors.*

Proof: A matrix in $DL_2(R_\sigma)$ has a determinant in $\mathbb{Z} \cap \mathbb{Z}[\sqrt{\sigma}]^\times = \{\pm 1\}$. It follows that a matrix in $DL_2(R_\sigma)$ sends primitive divectors to primitive divectors. For transitivity, consider a primitive red divector $(u, v\sqrt{\sigma})$. Since $\text{GCD}(u, \sigma v) = 1$, there exist $s, t \in \mathbb{Z}$ such that $su - tv\sigma = 1$. Observe that

$$\begin{pmatrix} u & t\sqrt{\sigma} \\ v\sqrt{\sigma} & s \end{pmatrix} \cdot \begin{pmatrix} 1 \\ 0 \end{pmatrix} = \begin{pmatrix} u \\ v\sqrt{\sigma} \end{pmatrix}.$$

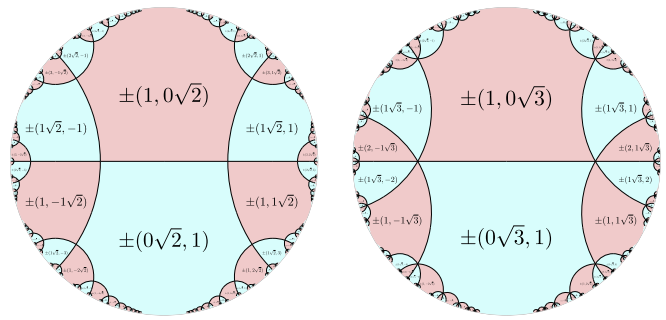


Fig. 5. The Coxeter geometries of type $(4, \infty)$ and $(6, \infty)$ are labeled by primitive lax divectors for $\mathbb{Z}[\sqrt{2}]$ and $\mathbb{Z}[\sqrt{3}]$, respectively. Around each point is a pinwheel.

Hence $DL_2^+(R_\sigma)$ acts transitively on the set of primitive red vectors. Since the matrix $\begin{pmatrix} 0 & 1 \\ -1 & 0 \end{pmatrix} \in DL_2(R_\sigma)$ swaps primitive red and blue divectors, the result follows. □

Define $PDL_2(R_\sigma) = DL_2(R_\sigma)/\{\pm 1\}$. When $\sigma = 2$ or $\sigma = 3$, Johnson and Weiss (ref. 9, section 4) present $PDL_2(R_\sigma)$ by generators and relations, proving the following.

Theorem 7. *If $\sigma = 2$ or $\sigma = 3$, then $PDL_2(R_\sigma)$ is isomorphic to the Coxeter group of type $(2\sigma, \infty)$.*

Explicitly, Johnson and Weiss (8) note that $PDL_2(R_\sigma)$ is generated by the triple of matrices (modulo ± 1),

$$s_1 = \begin{pmatrix} 0 & 1 \\ 1 & 0 \end{pmatrix}, s_2 = \begin{pmatrix} -1 & 0 \\ \sqrt{\sigma} & 1 \end{pmatrix}, s_3 = \begin{pmatrix} -1 & 0 \\ 0 & 1 \end{pmatrix},$$

which satisfy the Coxeter relations $s_1^2 = s_2^2 = s_3^2 = \pm 1$, $(s_1 s_2)^{2\sigma} = \pm 1$, $(s_1 s_3)^2 = \pm 1$. From their result, we were led to “dilinear” arithmetic interpretations of the geometries of types $(4, \infty)$ and $(6, \infty)$.

Arithmetic Flags. The “dilinear” variant of Conway’s topograph is as follows. Assume $\sigma = 2$ or $\sigma = 3$.

- Faces correspond to primitive lax divectors over R_σ , i.e., primitive divectors modulo ± 1 .
- Edges correspond to lax dibases: unordered pairs of lax divectors generating R_σ^2 as an R_σ module. This implies that the divectors are primitive, have opposite color, and form the rows of a matrix in $DL_2(R_\sigma)$.
- Points correspond to lax pinwheels: cyclically ordered 2σ -tuples of lax divectors such that any adjacent pair forms a lax dibasis (and hence has opposite color).

Theorem 8. *The geometry of primitive lax divectors, lax dibases, and pinwheels for R_σ is equivariantly isomorphic to the Coxeter geometry of type $(2\sigma, \infty)$ (Fig. 5).*

Binary Quadratic Diforms. Let us return to the general case of a square-free positive integer σ again. A binary quadratic diform (BQD) is a function of the form

$$Q(x, y) = ax^2 + b\sqrt{\sigma}xy + cy^2, \text{ where } a, b, c \in \mathbb{Z}.$$

We restrict (x, y) to be a divector in R_σ^2 , so the values of Q are integers. We define the discriminant of Q by $\Delta = \sigma(b^2\sigma - 4ac)$.

Restricting Q to red and blue divectors yields a pair $Q_{\text{red}}, Q_{\text{blue}}$ of BQFs over \mathbb{Z} of discriminant Δ ; explicitly,

$$Q_{\text{red}}(u, v) := Q(u, v\sqrt{\sigma}) = au^2 + b\sigma uv + cv^2,$$

$$Q_{\text{blue}}(u, v) := Q(u\sqrt{\sigma}, v) = a\sigma u^2 + b\sigma uv + cv^2.$$

This pair of BQFs can be related through an accessory form we call A_Δ . Namely, whenever $\sigma \mid \Delta$, define

$$A_\Delta(u, v) = \begin{cases} \sigma u^2 - \frac{\Delta}{4\sigma} v^2 & \text{if } \Delta\sigma^{-1} \equiv 0 \pmod{4}; \\ \sigma u^2 + \sigma uv - \frac{\Delta - \sigma^2}{4\sigma} v^2 & \text{if } \Delta\sigma^{-1} \not\equiv 0 \pmod{4}. \end{cases}$$

Write $\text{Cl}(\Delta)$ for the group of $SL_2(\mathbb{Z})$ -equivalence classes of primitive BQFs of discriminant Δ , following Bhargava (ref. 10, theorem 1). If Q is a BQF of discriminant Δ , write $[Q]$ for its $SL_2(\mathbb{Z})$ -equivalence class. Since A_Δ is an ambiguous form (its first coefficient divides its middle coefficient), its class in $\text{Cl}(\Delta)$ satisfies $[A_\Delta]^2 = 1$. The class of A_Δ has another characterization below.

Lemma 9. *If Q is a BQF of discriminant Δ that represents σ , and $\sigma \mid \Delta$, then $[Q] = [A_\Delta]$.*

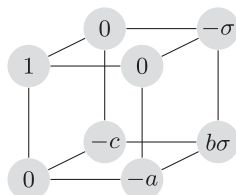
Proof: The square-freeness of σ is used repeatedly in what follows. If Q represents σ , then Q is $SL_2(\mathbb{Z})$ equivalent to a BQF of the form $\sigma u^2 + buv + cv^2$. Since $\sigma \mid \Delta = b^2 - 4\sigma c$, we find that $\sigma \mid b$. It follows that $\sigma u^2 + buv + cv^2$ is ambiguous and equivalent to $\sigma u^2 + \epsilon uv + kv^2$ for some $k \in \mathbb{Z}$ and $\epsilon \in \{0, 1\}$.

If $\epsilon = 0$, then $\Delta = -4\sigma k$ and $\Delta\sigma^{-1} \equiv 0 \pmod{4}$. In this case $k = -\Delta/4\sigma$. If $\epsilon = 1$, then $\Delta = \sigma^2 - 4\sigma k$ and $\Delta\sigma^{-1} \equiv \sigma - 4k \not\equiv 0 \pmod{4}$. In this case $k = -(\Delta - \sigma^2)/(4\sigma)$. \square

Thus, with σ fixed and $\sigma \mid \Delta$, we find that $[A_\Delta]$ is the unique class in $\text{Cl}(\Delta)$ which represents σ ; it happens to be a 2-torsion element in the class group. The following relates Q_{red} and Q_{blue} via A_Δ .

Theorem 10. *Suppose that a , $b\sigma$, and c are pairwise coprime. In $\text{Cl}(\Delta)$, one has $[Q_{\text{red}}] = [A_\Delta] \cdot [Q_{\text{blue}}]$. Conversely, if Q_1, Q_2 are primitive BQFs of discriminant Δ , and $\sigma \mid \Delta$, and $[Q_1] = [A_\Delta] \cdot [Q_2]$, there exists a BQD Q such that $[Q_{\text{red}}] = [Q_1]$ and $[Q_{\text{blue}}] = [Q_2]$.*

Proof: Consider the cube of integers below.



Let (M_i, N_i) be the partition of this cube into a pair of two-by-two matrices, in a front-back, left-right, and top-bottom fashion according to whether $i = 1, 2, 3$, respectively, as in ref. 10, section 2.1. From these matrices, Bhargava constructs a triple of binary quadratic forms $Q_i(u, v) = -\det(M_i u - N_i v)$:

$$\begin{aligned} Q_1(u, v) &= au^2 + b\sigma uv + c\sigma v^2; \\ Q_2(u, v) &= cu^2 + b\sigma uv + a\sigma v^2; \\ Q_3(u, v) &= \sigma u^2 + b\sigma uv + acv^2. \end{aligned}$$

By ref. 9, theorem 1, we have $[Q_1] \cdot [Q_2] \cdot [Q_3] = 1$ in $\text{Cl}(\Delta)$. Observe that Q_1 is precisely Q_{red} . Next, observe that Q_2 is related to Q_{blue} by switching u and v ; it follows that $[Q_2] = [Q_{\text{blue}}]^{-1}$. By Lemma 9, $[Q_3] = [A_\Delta]$. Since $[A_\Delta]^2 = 1$, we have

$$[Q_{\text{red}}] = [A_\Delta] \cdot [Q_{\text{blue}}] \text{ and } [Q_{\text{blue}}] = [A_\Delta] \cdot [Q_{\text{red}}].$$

For the converse, suppose that Q_1 and Q_2 are primitive BQFs of discriminant Δ , $\sigma \mid \Delta$, and $[Q_2] = [A_\Delta] \cdot [Q_1]$. Write $Q_1(u, v) = \alpha u^2 + \beta uv + \gamma v^2$, so $\sigma \mid \beta^2 - 4\alpha\gamma$. If $\sigma \mid \gamma$, then $\sigma \mid \beta$, and $Q_1 = Q_{\text{red}}$ for the diform

$$Q(x, y) = \alpha x^2 + \beta\sigma^{-1}\sqrt{\sigma}xy + \gamma\sigma^{-1}y^2.$$

If σ does not divide γ , then there exists an integer v satisfying the congruence $\alpha + \beta v + \gamma v^2 \equiv 0 \pmod{\sigma}$. One may check this by working one prime divisor of σ at a time; the quadratic formula applies for odd prime divisors. Modulo two, $2 \mid \sigma \mid \beta^2 - 4\alpha\gamma$ implies that β is even and the congruence has a solution.

Hence $Q_1(1, v) \equiv 0 \pmod{\sigma}$. Since Q_1 represents a multiple of σ , Q_1 is equivalent to a form $au^2 + \beta'uv + c\sigma v^2$. The fact that σ divides the discriminant implies $\beta' = b\sigma$ for some $b \in \mathbb{Z}$.

Thus, whether σ divides γ or not, $[Q_1] = [Q_{\text{red}}]$ for some diform Q . Since $[Q_2] = [A_\Delta] \cdot [Q_1]$, and $[Q_{\text{blue}}] = [A_\Delta] \cdot [Q_{\text{red}}]$, we find that $[Q_2] = [Q_{\text{blue}}]$. \square

Let $SDL_2^+(R_\sigma)$ be the subgroup of $DL_2^+(R_\sigma)$ consisting of matrices of determinant one. We say that two diforms Q, Q' are $SDL_2^+(R_\sigma)$ equivalent if there exists $\eta \in SDL_2^+(R_\sigma)$ satisfying $Q'(\vec{v}) = Q(\eta \cdot \vec{v})$ for all divectors \vec{v} . We write $[Q]_\sigma = [Q']_\sigma$ when the diforms Q and Q' are $SDL_2^+(R_\sigma)$ equivalent. One may check directly that $[Q]_\sigma = [Q']_\sigma$ implies $[Q_{\text{red}}] = [Q'_{\text{red}}]$ and $[Q_{\text{blue}}] = [Q'_{\text{blue}}]$. From this, we may reframe Theorem 10 in terms of equivalence classes.

Corollary 11. *Assume $\sigma \mid \Delta$. The map $Q \mapsto (Q_{\text{red}}, Q_{\text{blue}})$ yields a surjective function from*

- the set of $SDL_2^+(R_\sigma)$ -equivalence classes of binary quadratic diforms of discriminant Δ to...
- the set of ordered pairs $([Q_1], [Q_2])$ in $\text{Cl}(\Delta)$ satisfying $[Q_1] = [A_\Delta] \cdot [Q_2]$.

It seems interesting to determine the fibers of this map. As we will see, for $\sigma = 2$ and $\sigma = 3$, the question is how two of Conway's topographs can be interlaced in a single topograph of a diform.

Dilinear Topographs. Here we return to the assumption that $\sigma = 2$ or $\sigma = 3$. The topograph of a binary quadratic diform Q is obtained by replacing each primitive lax divector by the corresponding value of Q . Every value on the topograph of Q thus appears on the topograph of Q_{red} or of Q_{blue} . In this way, values from two of Conway's topographs interlace in the topograph of a binary quadratic diform. More precisely, we have the following.

Proposition 12. *If z appears on the topograph of Q_{red} , then (i) z appears on the topograph of Q or (ii) $\sigma \mid z$ and $z\sigma^{-1}$ appears on the topograph of both Q_{blue} and Q . Similarly, if z appears on the topograph of Q_{blue} , then (i) z appears on the topograph of Q or (ii) $\sigma \mid z$ and $z\sigma^{-1}$ appears on the topographs of both Q_{red} and Q .*

Proof: Suppose z occurs on the topograph of Q_{red} . Thus, $Q_{\text{red}}(u, v) = z$ for some coprime $u, v \in \mathbb{Z}$. If $\text{GCD}(u, \sigma v) = 1$, then $(u, v\sqrt{\sigma})$ is a primitive divector, and $Q(u, v\sqrt{\sigma}) = Q_{\text{red}}(u, v) = z$ appears on the topograph of Q .

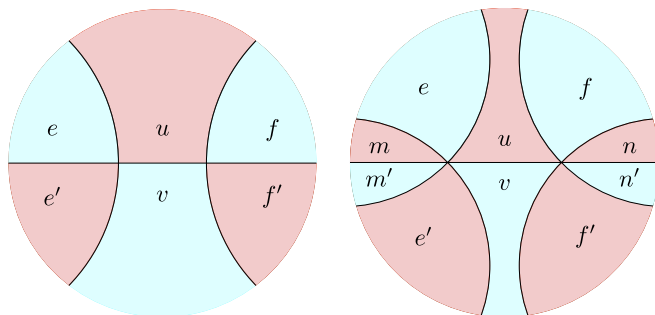


Fig. 6. Cells in the range topograph for $\sigma = 2$ (Left) and $\sigma = 3$ (Right).

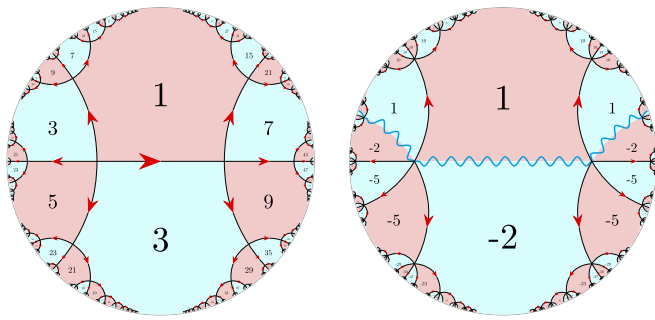


Fig. 7. Topographs for the definite binary quadratic diform $Q(x, y) = x^2 + \sqrt{2}xy + 3y^2$ over $\mathbb{Z}[\sqrt{2}]$ and the indefinite diform $Q(x, y) = x^2 - 2y^2$ over $\mathbb{Z}[\sqrt{3}]$.

If $\text{GCD}(u, \sigma v) \neq 1$, then $\sigma \mid u$ and $\text{GCD}(\sigma^{-1}u, v) = 1$. We compute $\sigma^{-1}z = \sigma^{-1}Q_{\text{red}}(u, v) = Q_{\text{blue}}(\sigma^{-1}u, v) = Q(\sigma^{-1}u\sqrt{\sigma}, v)$. Hence $\sigma^{-1}z$ appears on the topograph of both Q_{blue} and Q . \square

Corollary 13. Let μ_{red} and μ_{blue} be the minimum nonzero absolute values of Q_{red} and Q_{blue} . Then $\min\{\mu_{\text{red}}, \mu_{\text{blue}}\}$ is the minimum nonzero absolute value of Q .

The discriminant of a binary quadratic diform is locally visible in its topograph, according to the formulas below:

$$\Delta = \begin{cases} (2u - v)^2 - ef & \text{if } \sigma = 2; \\ (3u - v)^2 - ef = \frac{(4u - 3v)^2 - mn}{4} & \text{if } \sigma = 3. \end{cases} \quad [1]$$

Polarization for the quadratic form Q implies the following.

Theorem 14. At every cell in the topograph of Q , as in Fig. 6, one finds arithmetic progressions as below.

$\sigma = 2$: The triples $(e, 2u + v, f)$ and $(e', u + 2v, f')$ are arithmetic progressions of the same step size.

$\sigma = 3$: The triples $(e, 3u + v, f)$ and $(e', u + 3v, f')$ are arithmetic progressions of the same step size δ and the triples $(m, 4u + 3v, n)$ and $(m', 3u + 4v, n')$ are arithmetic progressions of the same step size 2δ .

Proof: In both cases $\sigma = 2, 3$, the integers e, u, v, f of a cell in Fig. 6 arise as values of Q of the form

$$e = Q(\sqrt{\sigma}\vec{v} - \vec{w}), u = Q(\vec{v}), v = Q(\vec{w}), f = Q(\sqrt{\sigma}\vec{v} + \vec{w}).$$

By the polarization identity for quadratic forms, the sequence

$$Q(\sqrt{\sigma}\vec{v} - \vec{w}), Q(\sqrt{\sigma}\vec{v}), Q(\sqrt{\sigma}\vec{v} + \vec{w})$$

is an arithmetic progression with step size $\delta := B_Q(\sqrt{\sigma}\vec{v}, \vec{w})$. Here B_Q is the bilinear form associated to the quadratic form Q . Similarly, the integers e', f' arise as values of Q :

$$e' = Q(\vec{v} - \sqrt{\sigma}\vec{w}), f' = Q(\vec{v} + \sqrt{\sigma}\vec{w}).$$

The sequence

$$Q(\vec{v} - \sqrt{\sigma}\vec{w}), Q(\vec{v}), Q(\vec{v} + \sqrt{\sigma}\vec{w})$$

is an arithmetic progression with step size $\delta' := B_Q(\vec{v}, \sqrt{\sigma}\vec{w})$. Note that $\delta = \delta'$, $Q(\sqrt{\sigma}\vec{v}) = \sigma u$, and $Q(\sqrt{\sigma}\vec{w}) = \sigma v$. Hence $(e, \sigma u + v, f)$ and $(e', u + \sigma v, f')$ are arithmetic progressions of the same step size.

When $\sigma = 3$, the values m, n arise as values of Q : $m = Q(2\vec{v} - \sqrt{3}\vec{w})$ and $n = Q(2\vec{v} + \sqrt{3}\vec{w})$. The polarization identity, applied again, shows that $(m, 4u + 3v, n)$ and $(m', 3u + 4v, n')$ are arithmetic progressions of the same step size 2δ . \square

Similar computations give linear relations among the values around any vertex in the topograph.



Proposition 15. (Refer to the vertex diagrams above.) When $\sigma = 2$, $a + c = b + d$. When $\sigma = 3$, $a + d = b + e = c + f$ and also $a + c + e = b + d + f$.

We draw an arrow on each edge to represent the direction of increasing progressions or a circle if all progressions are constant. Fig. 7 displays some examples. The climbing principle is the same as Conway's: Arrows always propagate when one looks at a cell of positive values. By the same argument as that of Conway, one obtains unique wells—a reduction theory for positive-definite diforms.

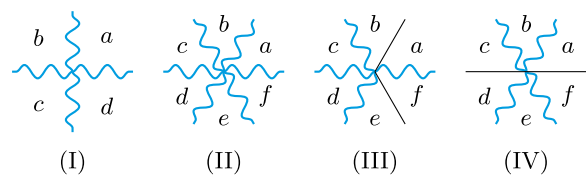
Proposition 16. Let Q be a positive-definite BQD over R_σ , with $\sigma = 2$ or $\sigma = 3$. Then the topograph of Q exhibits a unique well—either a single vertex or an edge (double well) from which all arrows emanate.

The river of a BQD is the set of segments separating positive values from negative ones in its topograph. The most interesting forms, just as for BQFs, are the nondegenerate indefinite forms.

Proposition 17. If Q is a nondegenerate indefinite diform, then its topograph contains a single endless nonbranching river.

Proof: The existence and uniqueness of a river follows from the same argument as for Conway's case. Namely, as one travels from a positive face to a negative face, one must at some point cross a river from positive to negative. This gives existence. The climbing principle (propagation of growth arrows) demonstrates that as one travels away from a river, one cannot hit another river, giving uniqueness. The crux of Proposition 17 is that rivers cannot branch.

For if a river branched, the faces around the branch point would alternate signs as they cross each river segment. Hence the rivers may branch only with even degree at a vertex. The possibilities, up to symmetry, are displayed below.



We apply Proposition 15 repeatedly. When $\sigma = 2$, the identity $a + c = b + d$ yields a contradiction if the signs of a and c are equal and opposite to the signs of b and d . Similarly, when $\sigma = 3$, the identity $a + c + e = b + d + f$ yields a contradiction if

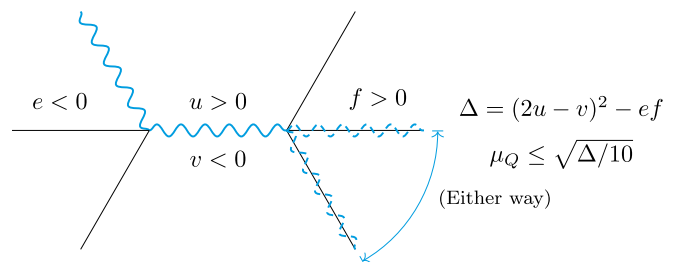


Fig. 8. Riverbend types for $\sigma = 2$.

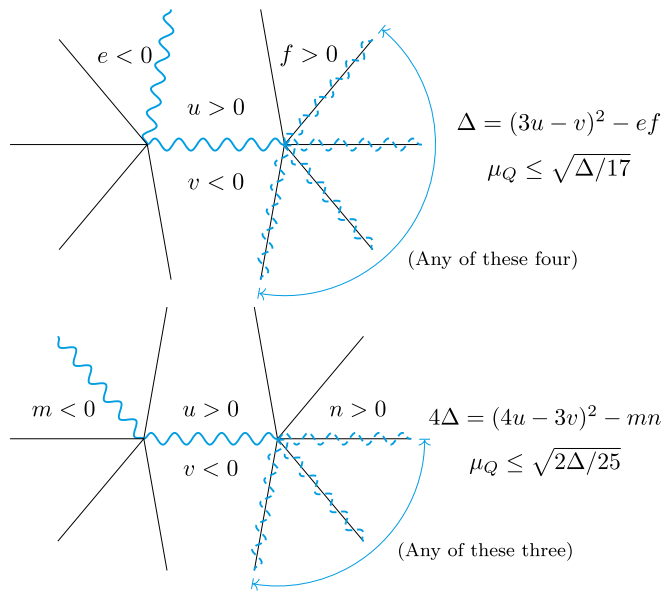


Fig. 9. Riverbend types for $\sigma = 3$.

the signs of a, c, e are equal and opposite to the signs of b, d, f . Branch-forms I and II are excluded.

It also happens that, when $\sigma = 3$, then $a + d = b + e = c + f$. Thus, we find a contradiction if the signs of a, d are equal and opposite to the signs of c, f . This excludes form III. We also find a contradiction if the signs of b, e are equal and opposite to the signs of a, d . This excludes form IV. Hence the river cannot branch. \square

As we have an endless nonbranching river, analysis of riverbends gives a minimum-value bound for diforms.

Theorem 18. Let Q be a nondegenerate indefinite BQD, and let μ_Q denote its minimum nonzero absolute value.

$\sigma = 2$: If Q is not $DL_2(R_\sigma)$ equivalent to a multiple of $x^2 - y^2$, then $\mu_Q \leq \sqrt{\Delta/10}$.

$\sigma = 3$: If Q is not $DL_2(R_\sigma)$ equivalent to a multiple of $x^2 - y^2$, then $\mu_Q \leq \sqrt{2\Delta/25}$.

Proof: The entire river cannot be adjacent to a single region, because its values opposite such a region would form a biinfinite quadratic sequence with positive sign and negative acceleration or negative sign and positive acceleration. Hence the river must “bend.” If one finds riverbends as in Figs. 8 and 9, Eq. 1 gives the stated minimum value bound or better (as derived in Figs. 8 and 9). If no such riverbends of those shapes occur, then the river must maintain one of the three shapes of Fig. 10 throughout its entire length.

The isometry group of such a homogeneous river includes a translation along the river. Replacing Q by a $DL_2(R_\sigma)$ -equivalent form if necessary, we may place this river through the segment separating $\pm(1, 0)$ and $\pm(0, 1)$. Translation along the homogeneous rivers is then given by the matrices

$$R = \begin{pmatrix} \sqrt{2} & 1 \\ 1 & \sqrt{2} \end{pmatrix}, S = \begin{pmatrix} 2 & \sqrt{3} \\ \sqrt{3} & 2 \end{pmatrix}, T = \begin{pmatrix} \sqrt{3} & 2 \\ 1 & \sqrt{3} \end{pmatrix}$$

in the three cases shown in Fig. 10. Periodicity of the river implies that R^e, S^e , or T^e is an isometry of Q for some $e > 0$.

The eigenvectors of R and S are $(1, 1)$ and $(1, -1)$. If λ and μ denote their eigenvalues, then

$$Q(1, 1) = \lambda^{2e} Q(1, 1) \text{ and } Q(1, -1) = \mu^{2e} Q(1, -1).$$

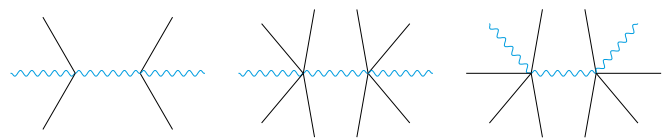


Fig. 10. One more river shape for $\sigma = 2$ and two more shapes for $\sigma = 3$.

But a quick computation demonstrates that $\lambda, \mu \in \mathbb{R}$ and $\lambda, \mu \notin \{1, -1\}$. Hence $Q(1, 1) = Q(1, -1) = 0$ in the two straight-river cases. Writing the diform as $Q(x, y) = ax^2 + b\sqrt{\sigma}xy + cy^2$, this implies $a + b\sqrt{\sigma} + c = a - b\sqrt{\sigma} + c = 0$. Hence $a = -c$ and $b = 0$. We have proved that an endless straight river occurs only if Q is equivalent to a multiple of $x^2 - y^2$ (when $\sigma = 2$ or $\sigma = 3$).

It remains to study the third shape of the homogeneous river, on which T acts by translation. The eigenvectors of T are $(\sqrt{2}, \pm 1)$, with eigenvalues $\sqrt{3} \pm \sqrt{2}$, respectively. Hence, if T^e is an isometry of Q for some $e > 0$, then $Q(\sqrt{2}, 1) = Q(\sqrt{2}, -1) = 0$. In this case, $2a + b\sqrt{6} + c = 2a - b\sqrt{6} + c = 0$. Hence $b = 0$ and $c = -2a$. We have proved that an endless homogeneous river of the third form occurs if and only if Q is equivalent to a multiple of $x^2 - 2y^2$ (displayed in Fig. 7). The discriminant of the diform $x^2 - 2y^2$ is 24, while its minimum absolute value is $\mu_Q = 1$. The estimate $\mu_Q \leq \sqrt{2\Delta/25}$ can be directly checked in this case, finishing the proof. \square

The discriminant of the diform $x^2 - y^2$ is 4σ and its minimal value is $\mu_Q = 1$. Thus, when $\sigma = 2$, the estimate $\mu_Q \leq \sqrt{\Delta/10}$ is violated; when $\sigma = 3$, the estimate $\mu_Q \leq \sqrt{2\Delta/25}$ is violated. Hence the exceptional diforms $x^2 - y^2$ cannot be removed from Theorem 18.

Corollary 19. Suppose that Q_1 and Q_2 are nondegenerate indefinite BQFs of discriminant Δ , with $\sigma \mid \Delta$ and $[Q_2] = [A_\Delta] \cdot [Q_1]$. Then

$\sigma = 2$: If Q_1 and Q_2 are not equivalent to a multiple of $x^2 - 2y^2$, then $\min\{\mu_{Q_1}, \mu_{Q_2}\} \leq \sqrt{\Delta/10}$.

$\sigma = 3$: If Q_1 and Q_2 are not equivalent to a multiple of $x^2 - 3y^2$, then $\min\{\mu_{Q_1}, \mu_{Q_2}\} \leq \sqrt{\Delta/13}$.

Proof: This follows directly from Theorems 18 and 10, except that $2/25$ has been replaced by $1/13$. This replacement is possible, due to a gap in the Markoff spectrum between $\sqrt{12}$ and $\sqrt{13}$; see ref. 11, section 1, proof of theorem 3.3. \square

4. Conclusion

In each of the discussed examples, there is a coincidence between a Coxeter group and an arithmetic group. For Conway’s topograph, it is the coincidence between the Coxeter group of type $(3, \infty)$ and the arithmetic group $PGL_2(\mathbb{Z})$. The dilinear groups, of Coxeter types $(2\sigma, \infty)$ for $\sigma = 2, 3$, are arithmetic subgroups of $PGU_{1,1}^{\mathbb{Q}(\sqrt{\sigma})/\mathbb{Q}}(\mathbb{Q})$, the projective unitary similitude group for a Hermitian form relative to $\mathbb{Q}(\sqrt{\sigma})/\mathbb{Q}$.

Table 1. Commensurability classes of simplicial hyperbolic arithmetic Coxeter groups of dimension at least 3 (extracted from ref. 19)

Dimension	Coxeter types
3	(3, 3, 6) and (3, 4, 4)
4	(3, 3, 3, 5) and (3, 3, 3, 4) and (3, 4, 3, 4)
5	(3, 3, 3, 4, 3) and (3, 3 ^[5])
6	(4, 3 ² , 3 ^{2,1}) and (3, 3 ^[6])
7	(3 ^{2,2,2}) and (4, 3 ³ , 3 ^{2,1}) and (3, 3 ^[7])
8	(3 ^{4,3,1})
9	(3 ^{6,2,1})

When such a coincidence occurs, the Coxeter group is arithmetic, and the following two questions are natural.

- i) Is there an arithmetic interpretation for the flags in the Coxeter group?
- ii) Does the Coxeter geometry give a new reduction theory for a class of quadratic (or Hermitian) forms?

The first question is reminiscent of the classical theory of flag varieties. When G is a simple simply connected linear algebraic group over a field k , one can often identify a “standard” representation of G on a k -vector space V . Every k -parabolic subgroup of G is the stabilizer of some sort of k flag in V . If G is a symplectic or spin or unitary group, these are the isotropic flags in the standard representation. In type G_2 , these are the nil flags in the split octonions. In an 11-part series of papers (*Beziehungen der \mathcal{E}_7 und \mathcal{E}_8 zur Oktavenebene I–XI*, published 1954–1963, refs. 12–16), Freudenthal studied the “metasymplectic” geometry which describes flags in representations of exceptional groups.

Now it appears that arithmetic Coxeter groups provide a parallel industry, examining their representations on various modules over Euclidean domains. Arithmetic flags are generalized bases of these modules. The geometry of arithmetic flag varieties seems (so far) to be the combinatorial geometry of Coxeter groups. We do not yet see algebraic geometry in the picture, as one finds in flag varieties G/P .

The applications to arithmetic (the arithmetic of arithmetic Coxeter groups) include Conway’s approach to binary quadratic forms and new generalizations. The reduction theory for quadratic and Hermitian forms is a classical subject, sometimes tedious in its algebra—the Coxeter geometry and Conway’s theory of wells and rivers give an intuitive approach. Beyond reframing old results, it seems unlikely that one would find the reduction theory of our “diforms” (or suitable pairs of binary quadratic forms) without considering the Coxeter group. In this way, arithmetic Coxeter groups offer applications to number theory.

This paper has discussed five arithmetic Coxeter groups, of types $(3, \infty)$, $(3, 3, 6)$, $(3, 4, 4)$, $(4, \infty)$, and $(6, \infty)$. If this is a game of coincidences, when might it end? In ref. 17, Belolipetsky surveys the arithmetic hyperbolic Coxeter groups; following his treatment, we review the classification of such Coxeter groups.

The groups we have studied are simplicial hyperbolic arithmetic Coxeter groups. In ref. 18, Vinberg proves there are 64 such groups in dimension at least 3. These fall into 14 commensurability classes by ref. 19, as shown in Table 1. It would not be surprising if each one offered a notion of arithmetic flags (e.g., superbases, etc.) and quadratic/Hermitian forms. For example, the Coxeter group of type $(3, 3, 3, 4, 3)$ is arithmetic, commensurable with $PGL_2(A)$ where A is the Hurwitz order in the quaternion algebra $\mathbb{Q} + \mathbb{Q}i + \mathbb{Q}j + \mathbb{Q}k$. Arithmetic flags in this case can be interpreted as lax vectors, bases, superbases, 3-simplex bases, 4-simplex bases, and 5-orthoplex bases, in the A -module A^2 .

Table 1 displays only groups of dimension at least 3. In dimension 2, we find Conway’s topograph and its dilinear variants. One might also consider arithmetic hyperbolic triangle groups, classified by Takeuchi in refs. 20 and 21. Up to commensurability, there are 19 of these, each associated to a quaternion algebra over a totally real field. Vertices, edges, and triangles in the resulting hyperbolic tilings surely correspond to arithmetic objects—What are they?

If one wishes to depart from the simplicial groups, there are nonsimplicial arithmetic hyperbolic Coxeter groups. In the results of Vinberg (22), all examples occur in dimension at most 30; there are finitely many up to commensurability. One may be able to explore the arithmetic of arithmetic Coxeter groups for a long time—what is currently missing is a general theory of arithmetic flags and forms to make predictions in a less ad hoc manner.

Departing from the setting of Coxeter groups may also be appealing, especially in low dimension. For example, the Coxeter geometry makes the reduction theory of BHF’s particularly appealing over $\mathbb{Z}[i]$ and $\mathbb{Z}[\omega]$. But Bestvina and Savin (7) are able to work over other quadratic imaginary rings although the geometry lacks homogeneity. One might study diforms over other real quadratic rings, in the same way. More arithmetic may be found in “thin” rather than arithmetic groups, e.g., in the work of Stange (23) on Apollonian circle packings. Still, Coxeter groups seem an appropriate starting place, where arithmetic applications are low-hanging fruit.

ACKNOWLEDGMENTS. The authors thank the anonymous referee for comments and insights. M.H.W. is supported by the Simons Foundation Collaboration Grant 426453.

1. Conway JH (1997) *The Sensual (Quadratic) Form*. Carus Mathematical Monographs (Mathematical Association of America, Washington, DC), Vol 26.
2. Gauss CF (1986) *Disquisitiones Arithmeticae*, trans Clarke AA, revised by Waterhouse WC, Greither C, and Grootendorst AW (Springer, New York).
3. Bianchi L (1891) Geometrische darstellung der gruppen linearer substitutionen mit ganzen complexen coefficienten nebst anwendungen auf die zahlentheorie [Geometric representation of groups of linear substitutions with complex coefficients and applications to number theory]. *Math Ann* 38:313–333.
4. Fricke R, Klein F (1897) *Vorlesungen über die Theorie der Automorphen Functionen* [Lectures on the theory of automorphic functions] (B. G. Teubner, Leipzig, Germany), Vol 1.
5. Schulte E, Weiss AI (1994) Chirality and projective linear groups. *Discrete Math* 131:221–261.
6. Coxeter HSM (1973) *Regular Polytopes* (Dover Publications, Inc., New York), 3rd Ed.
7. Bestvina M, Savin G (2012) Geometry of integral binary Hermitian forms. *J Algebra* 360:1–20.
8. Shelley CD (2013) An arithmetic construction of the Gaussian and Eisenstein topographs. PhD thesis (University of California, Santa Cruz, CA).
9. Johnson NW, Weiss AI (1999) Quadratic integers and Coxeter groups. *Canad J Math* 51:1307–1336.
10. Bhargava M (2004) Higher composition laws. I. A new view on Gauss composition, and quadratic generalizations. *Ann Math* 159:217–250.
11. Hall M, Jr (1971) The Markoff spectrum. *Acta Arith* 18:387–399.
12. Freudenthal H (1954) Beziehungen der \mathcal{E}_7 und \mathcal{E}_8 zur Oktavenebene [Relationship of \mathcal{E}_7 and \mathcal{E}_8 with the Cayley plane], I–II. *Nederl Akad Wetensch Proc Ser A* 57:218–230; 363–368.
13. Freudenthal H (1955) Beziehungen der \mathcal{E}_7 und \mathcal{E}_8 zur Oktavenebene [Relationship of \mathcal{E}_7 and \mathcal{E}_8 with the Cayley plane], III. *Nederl Akad Wetensch Proc Ser A* 58:151–157.
14. Freudenthal H (1955) Beziehungen der \mathcal{E}_7 und \mathcal{E}_8 zur Oktavenebene [Relationship of \mathcal{E}_7 and \mathcal{E}_8 with the Cayley plane], IV. *Nederl Akad Wetensch Proc Ser A* 58:277–285.
15. Freudenthal H (1959) Beziehungen der \mathcal{E}_7 und \mathcal{E}_8 zur Oktavenebene [Relationship of \mathcal{E}_7 and \mathcal{E}_8 with the Cayley plane], V–IX. *Nederl Akad Wetensch Proc Ser A* 62:165–201, 447–474.
16. Freudenthal H (1963) Beziehungen der \mathcal{E}_7 und \mathcal{E}_8 zur Oktavenebene [Relationship of \mathcal{E}_7 and \mathcal{E}_8 with the Cayley plane], X–XI. *Nederl Akad Wetensch Proc Ser A* 66:455–487.
17. Belolipetsky M (2016) Arithmetic hyperbolic reflection groups. *Bull Am Math Soc* 53:437–475.
18. Vinberg EB (1967) Discrete groups generated by reflections in Lobachevskii spaces. *Math USSR Sbornik* 1:429–444.
19. Johnson NW, Kellerhals R, Ratcliffe JG, Tschantz ST (2002) Commensurability classes of hyperbolic Coxeter groups. *Linear Algebra Appl* 345:119–147.
20. Takeuchi K (1977) Commensurability classes of arithmetic triangle groups. *J Fac Sci Univ Tokyo Sect IA Math* 24:201–212.
21. Takeuchi K (1977) Arithmetic triangle groups. *J Math Soc Jpn* 29:91–106.
22. Vinberg EB (1981) The nonexistence of crystallographic reflection groups in Lobachevskii spaces of large dimension. *Funktional Anal i Prilozhen* 15:67–68.
23. Stange KE (2016) The sensual Apollonian circle packing. *Expo Math* 34:364–395.